Invited Paper

Excitation of terahertz plasmon in two-dimensional electron gas

Hua Qin [1*], Yao Yu [1, 2], Xiang Li [1, 2], Jiandong Sun [1], and Yongdan Huang [1]
[1] Key Laboratory of Nanodevices and Applications,
Suzhou Institute of Nano-tech and Nano-bionics (SINANO), Chinese Academy of Sciences,
398 Ruoshui Road, Suzhou 215123, P. R. China
[2] Graduate University of Chinese Academy of Sciences, Beijing 100049, P. R. China
[*1] Email: hqin2007@sinano.ac.cn

(Received June 23，2016)

Abstract: High-speed electronics is marching towards terahertz frequency regime in which electronics and optoelectronics are merging into a new realm. Efficient solid-state terahertz emitters/oscillators and high-speed high-sensitivity detectors are the most important active devices for terahertz applications. In the frequencies ranging from 1 *THz* to 3 *THz*, both electronic and photonic devices become less efficient. As coherent collective charge oscillations in the terahertz frequency range, plasmon in two-dimensional electron gas (2DEG) has long been pursued for active solid-state terahertz devices, especially emitters. However, such emitters are not yet practical since the conversion efficiency is yet lower than 10^{-3}. In this review, we present excitation and probing of localized plasmon modes in grating-coupled and antenna-coupled field-effect transistors based on AlGaN/GaN heterostructures. It is shown that the damping of plasmons remains the critical problem in developing practical terahertz plasmon emitters. Nevertheless, non-resonant excitation of terahertz plasmons in antenna-coupled 2DEG is enabling a technology for high sensitivity detection of terahertz electromagnetic wave at room temperature.

Keywords: Plasmon, Two-dimensional electron gas, Terahertz detector, Terahertz emitter, Terahertz modulator

doi: 10.11906/TST.71-81.2016.06.07

1. Introduction

The advance of terahertz science and technology relies on the development of efficient terahertz sources and high sensitivity detectors [1]. The physics of wave-particle interactions in solid-state electronic system and the effective manipulation of such interactions are the key in realizing efficient active terahertz devices. Unlike in vacuum electronics in which electrons could be accelerated to a relativistic speed, the drift velocity of electrons in solid-state electronics is limited by a saturation velocity due to strong scattering by phonons, impurities and etc. However, electrons in solid-state devices can be well confined in a conduction channel and the interaction with both terahertz electromagnetic wave and electrostatic field can be controlled by using various methods, such as field-effect gate, antenna, grating coupler and terahertz cavity [2-6]. Many ideas of wave-particle interaction implemented in microwave/millimeter-wave vacuum electronics could be borrowed for solid-state terahertz electronics [7, 8]. Especially when plasma wave as a collective excitation in 2DEG instead of single-particle excitation is considered, the coupling between terahertz electromagnetic wave and plasma wave plays an important role in facilitating the efficiency of terahertz emission and detection.

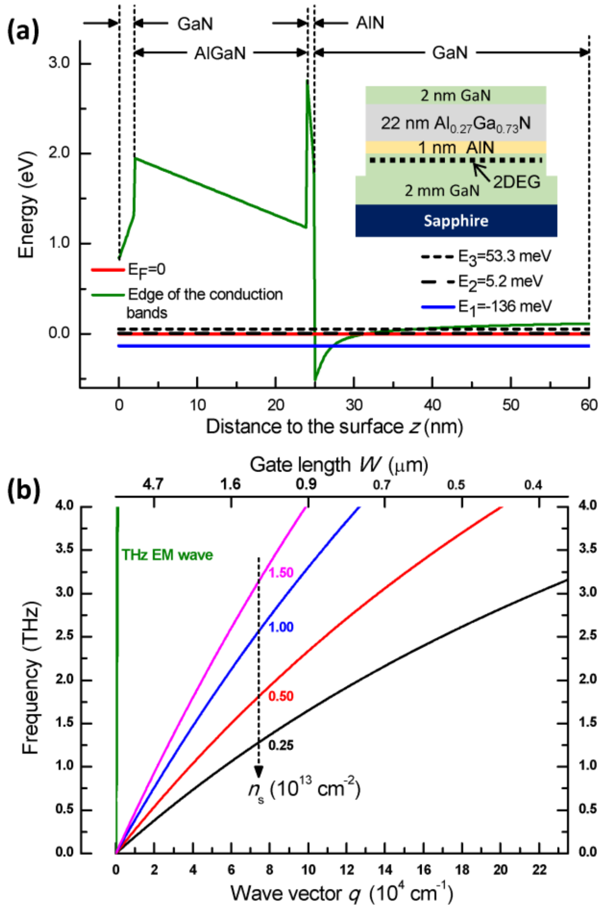

Fig. 1 (a) Conduction-band diagram of an AlGaN/GaN heterostructure from a self-consistent calculation. The 2DEG is formed in the GaN quantum well where

Plasmons in 2DEG have long been considered for active media of terahertz emitters. It was proposed that plasmons excited by electron transport emit terahertz electromagnetic wave into a free space by using a grating coupler or antenna [2, 3, 7-16]. The main hurdles for this approach are two folds. The efficiency of plasmon excitation by drifting electrons is low since the required drift velocity is close to or even higher than the Fermi velocity or the saturation velocity [14]. The other limiting factor is that the plasmons excited in 2DEG are highly dissipative due to the scattering and the electrostatic coupling to the nearby electron gas. Similarly, such dissipation of plasmons is the limiting factor for high sensitivity terahertz detection too. Hence, the engineering of plasmon system is necessary to realize any efficient terahertz device. Here in this review, we present preliminary results on the excitation and probing of terahertz plasmons in two different types of 2DEG devices attempting to realize high efficiency terahertz emission and high sensitivity detection.

2. Experimental methods

The 2DEG utilized in this study is realized in an AlGaN/GaN heterostructure grown by MOCVD method on a sapphire substrate. A self-consistent calculation shows that there are two lowest sub levels are occupied by free electrons in the GaN quantum well at room temperature as shown in Fig. 1(a). The electron density (n_s) and the mobility (μ) are 1×10^{13} cm^{-2} and 1800 cm^2/Vs at 300 *K*, respectively. At lower temperatures below 77 *K*, the mobility is increased up to 15,000 cm^2/Vs while the electron density is kept fairly constant. The choice of AlGaN/GaN instead of AlGaAs/GaAs which could provide an even higher electron mobility has three aspects. First of all, the electron density in AlGaN/GaN is usually one order of magnitude higher than that in AlGaAs/GaAs heterostructures. Plasmon in AlGaN/GaN 2DEG can thus be tuned in a wider frequency range (up to 6 *THz*), as shown in Fig. 1(b), either by varying the electron density or by defining the geometric dimension (e.g., the gate length W) of the 2DEG. Secondly, the 2DEG in AlGaN/GaN is much closer ($d = 25$ nm) to the surface than that (typically more than 45 *nm*) in AlGaAs/GaAs. Such a close distance to the surface on which field-effect gate and grating coupler are made helps to enhance the terahertz near-field strength and hence the coupling strength between the 2DEG and the terahertz electromagnetic wave. It is the strong spontaneous polarization in AlGaN/GaN heterostructure that results in high electron density and high mobility without the need of intentional doping in the AlGaN barrier layer. Finally, the tunneling current between the gate and the 2DEG can be manipulated. It can be suppressed by inserting a dielectric layer such as Al_2O_3 grown by atomic-layer-deposition between the heterostructure and the gate. On the other hand, it can be enhanced by defects and impurities in AlGaN barrier layer so that injection of electron from the gate into the 2DEG for plasmon excitation becomes possible.

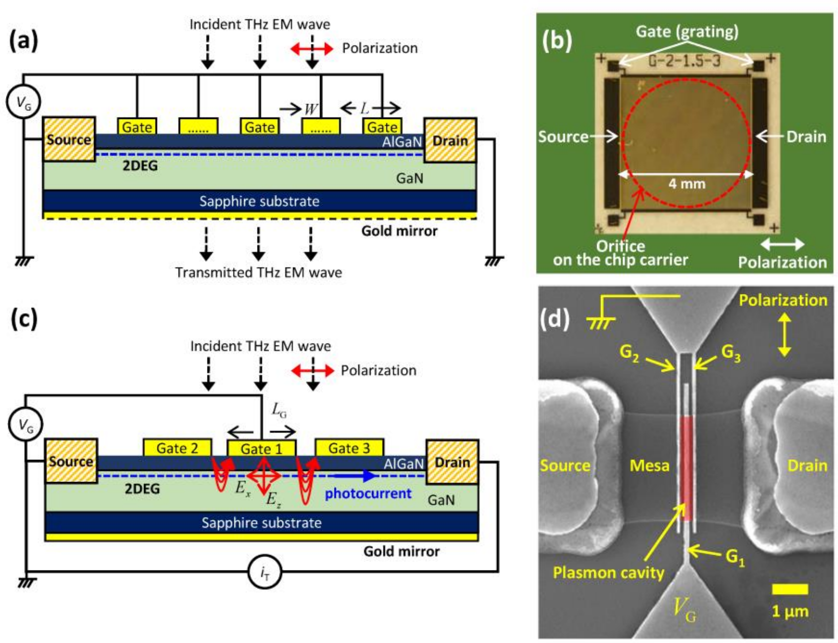

Fig. 2 (a) Schematic and (b) micrograph of the grating-coupled field-effect transistor. (c) Schematic and (d) micrograph of the antenna-coupled field-effect transistor.

Two devices namely the grating-coupled field-effect transistor and the antenna-coupled field-effect transistor are designed and fabricated. The grating-coupled device is designed so that a large-area field-effect 2DEG allows for probing of plasmons excited by an incident terahertz wave. The device also allows for probing any possible terahertz emission from the 2DEG in which plasmons are excited by an injection current. The grating-coupled field-effect transistor is schematically shown in Fig. 2(a) and the micrograph is shown in Fig. 2(b). Each gate has a length about $W = 2.7\ \mu\mathrm{m}$ and the grating gates have a pitch distance of $L = 4\ \mu\mathrm{m}$. By applying a negative gate voltage V_G, the electron density under the grating can be modulated periodically and individual plasmon cavities are thus defined. Similar devices have been studied by using 2DEG from AlGaAs/GaAs heterostructures and others which have the advantage of higher electron mobility [2, 3, 12, 16, 17]. The area of the grating-coupled 2DEG is 4 *mm* by 4 *mm*. The device was mounted on two different chip carriers. When it is mounted on a chip carrier with a central orifice with a diameter of 4 *mm*, the device can be characterized by measuring the terahertz transmission spectra at different gate voltages. On the other hand, terahertz plasmon emission spectra can be measured when the device is mounted on a gold-plated chip carrier which provides a reflective mirror on the backside of the sapphire substrate. The antenna-coupled field-effect transistor consists of two antenna blocks each of which is of a dipole antenna, as shown in Fig. 2 (c, d). One of the antennas provides a central gate G_1 with a gate length of 150 *nm* and the other provides two gates (G_2 and G_3, both have a length of 100 *nm*) surrounding gate G_1. The inner distance between G2 and G3 is 330 *nm*. Only gate G_1 is applied with an external gate voltage V_G. Other two gates are connected to ground, as shown in Fig. 2(d).

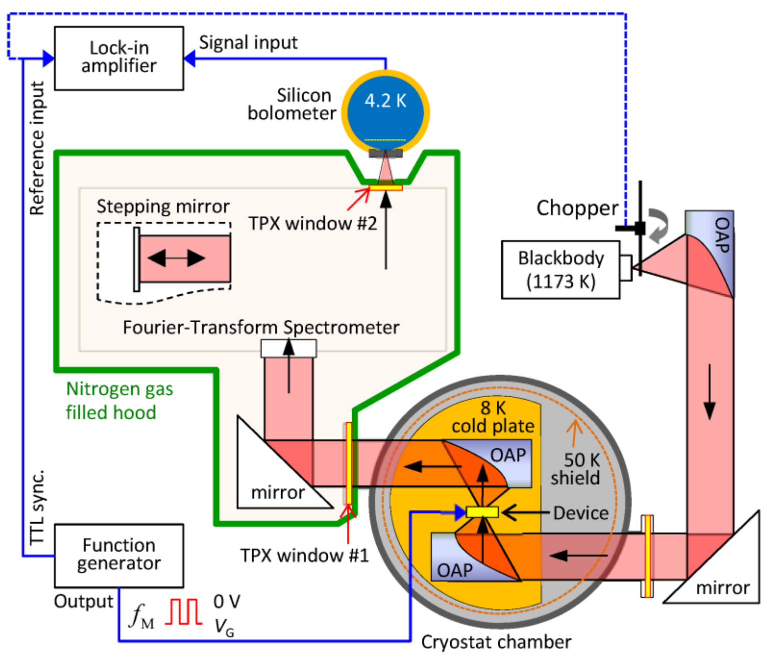

Fig. 3 Schematic of the setup allowing for measurement of the transmission, emission spectra and photocurrent response

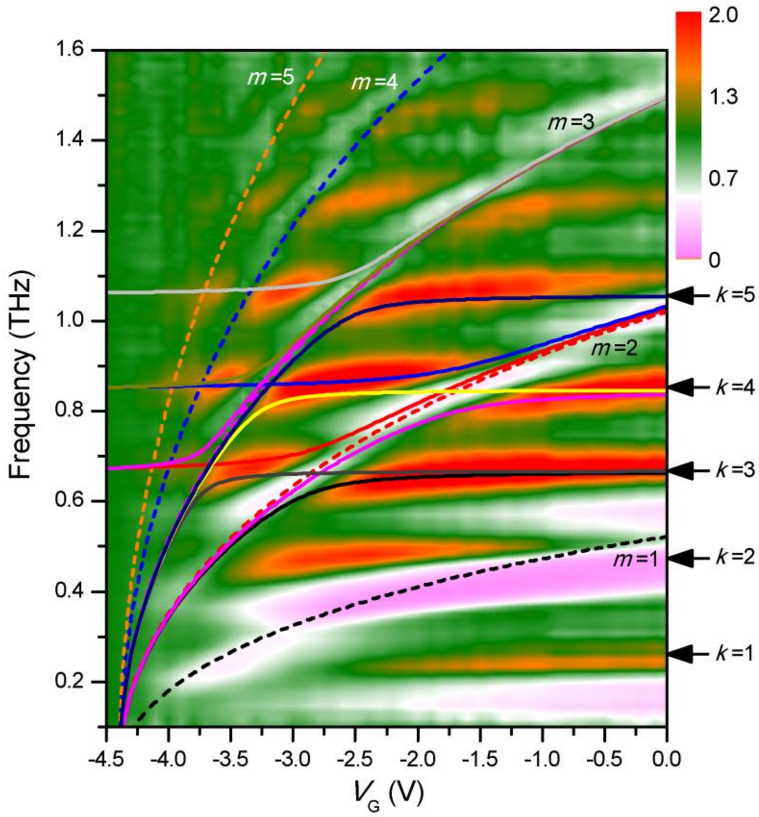

Fig. 4 Transmission spectra at different gate voltages obtained from the grating-coupled field-effect transistor cooled down to 8 *K*. The spectra were measured using a terahertz time-domain spectrometer (THz-TDS). Refer to Ref. 18 for the same measurement setup. Similar transmission spectra (worse signal-to-noise ratio comparing to the THz-TDS data) were obtained by using setup shown in Fig. 3.

To probe any possible plasmon excited in the gated 2DEG, terahertz transmission spectra, emission spectra and terahertz photocurrent (i_T) at different gate voltages (i.e., different electron densities/plasmon frequencies) are experimentally studied. For these purposes, a cryogenic vacuum chamber was designed and constructed allowing for cooling the devices down to 7 *K*. As shown in Fig. 3, the chamber offers two terahertz windows made of transparent polymethylpentene (TPX) so that terahertz wave can be transmitted through the device under test. Also the setup allows for testing the terahertz emission from and the photocurrent in the device. To detect and analyze the terahertz electromagnetic wave emitted from or transmitted through the device, a Fourier-transform spectrometer equipped with a liquid-helium-cooled silicon bolometer is used. Both in the emission and transmission experiments, the gate voltage applied to the grating-coupled device is in a square-wave form whose high level is fixed at 0 *V* while the low level (also termed as V_G) is continuously tunable from -25 *mV* to -5 *V*. The duty cycle is fixed at 50% and the frequency is fixed at 317*Hz*. A lock-in amplifier following the silicon bolometer reads out the terahertz power. In the photocurrent experiment (setup not shown in Fig. 3. Refer to Ref. [19-22] for details), a tunable coherent terahertz source is used to excite the device and the induced photocurrent or photovoltage is amplified and measured. In this case, the terahertz source can be modulated either externally by a mechanical chopper or internally by a TTL signal. The same lock-in amplifier is used to read out the photoresponse which is amplified first by a low-noise current preamplifier or a low-noise voltage preamplifier.

3. Plasmon excitation in a grating-coupled 2DEG

Plasmons excited in AlGaN/GaN 2DEG is examined in the grating-coupled field-effect transistor by measuring the terahertz transmission spectra at different gate voltages, as shown in Fig. 4. Rich features are observed. Strong suppression in terahertz transmission are marked by 5 dashed curves corresponding to the first 5 plasmon modes ($m = 1, 2, 3, 4$ and 5) controlled by the gate voltage, i.e., the localized plasmon modes under the grating gates. These discretized plasmon modes can be well described by the dispersion relation [3]

$$\omega_{\mathrm{P}m} = \sqrt{\frac{n_{\mathrm{s}} e^2}{2m^* \varepsilon_0 \bar{\varepsilon}} q_m}\ , \tag{1}$$

where, $\omega_{\mathrm{P}m}$ and $q_m = m\pi / W$ are the angular frequency and the wave number of the plasmon mode, e is the elementary electron charge, $m^* = 0.2m_0$ is the effective electron mass for AlGaN/GaN 2DEG, ε_0 and $\bar{\varepsilon}$ are the vacuum permittivity and the relative permittivity of the 2DEG. The gate controlled electron density can be approximated as $n_{\mathrm{s}} = C_{\mathrm{G}}(V_{\mathrm{G}} - V_{\mathrm{T}}) / e$, where $C_{\mathrm{G}} \approx \varepsilon_0 \varepsilon_{\mathrm{AlGaN}} / d \simeq 0.34\ \mu\mathrm{F/cm}^2$ is the gate capacitance per unit area, $V_{\mathrm{T}} \approx -4.4\ \mathrm{V}$ is the threshold gate voltage to deplete the 2DEG, $\varepsilon_{\mathrm{GaN}} = 9.7$ and $\varepsilon_{\mathrm{AlGaN}} = 9.5$ are the relative permittivity for GaN and AlGaN, respectively. For the grating-coupled 2DEG, the relative permittivity $\bar{\varepsilon}$ can be approximated by taking into account the 2DEG areas screened and unscreened by the grating gates

$$\begin{aligned} \bar{\varepsilon} &= W\bar{\varepsilon}_{\mathrm{screened}} / L + (1 - W/L)\bar{\varepsilon}_{\mathrm{unscreened}}, \\ \bar{\varepsilon}_{\mathrm{screened}} &= \frac{1}{2}\left[\varepsilon_{\mathrm{GaN}} + \varepsilon_{\mathrm{AlGaN}} \coth(q_m d)\right], \\ \bar{\varepsilon}_{\mathrm{unscreened}} &= \frac{1}{2}\left[\varepsilon_{\mathrm{GaN}} + \varepsilon_{\mathrm{AlGaN}} \frac{1 + \varepsilon_{\mathrm{AlGaN}} \tanh(q_m d)}{\varepsilon_{\mathrm{AlGaN}} + \tanh(q_m d)}\right]. \end{aligned} \tag{2}$$

As shown in Fig. 4, strong transmission can be found at a few equally-spaced frequencies (marked by $k = 1, 2, 3, 4, 5$) corresponding to the eigen modes of the sapphire Fabry-Pérot cavity

$$\omega_k = k \frac{\pi c}{\bar{n} D} \tag{3}$$

where, $k = 1, 2, 3, \ldots$ is the cavity mode number, c is the speed of light in vacuum, $\bar{n} \approx 3.0$ and $D = 238\ \mu\text{m}$ are the effective refractive index and the length of the cavity. A pair of strongly coupled terahertz cavity mode and plasmon mode hybridizes into an upper (ω_{km}^{+}) and a lower (ω_{km}^{-}) plasmon-polariton state [18, 19]

$$\omega_{km}^{\pm} = \frac{\omega_k + \omega_{\mathrm{P}m}}{2} - \frac{j}{2}(\gamma_{\mathrm{C}} + \gamma_{\mathrm{P}}) \pm \frac{1}{2}\sqrt{(\delta\omega)^2 + 4V_{km}^2 - (\gamma_{\mathrm{C}} - \gamma_{\mathrm{P}})^2 - 2j(\gamma_{\mathrm{C}} - \gamma_{\mathrm{P}})\delta\omega}, \tag{4}$$

where $\delta\omega = \omega_k - \omega_{\mathrm{P}m}$ is the detuning of the plasmon mode from the terahertz cavity mode, V_{km} is the coupling strength, γ_{P} is the linewidth of the plasmon mode, and γ_{C} is the linewidth of the terahertz cavity mode. The solid curves in Fig. 4 are calculated plasmon-polariton modes based on Eq. 4 and agree well with the experiment data.

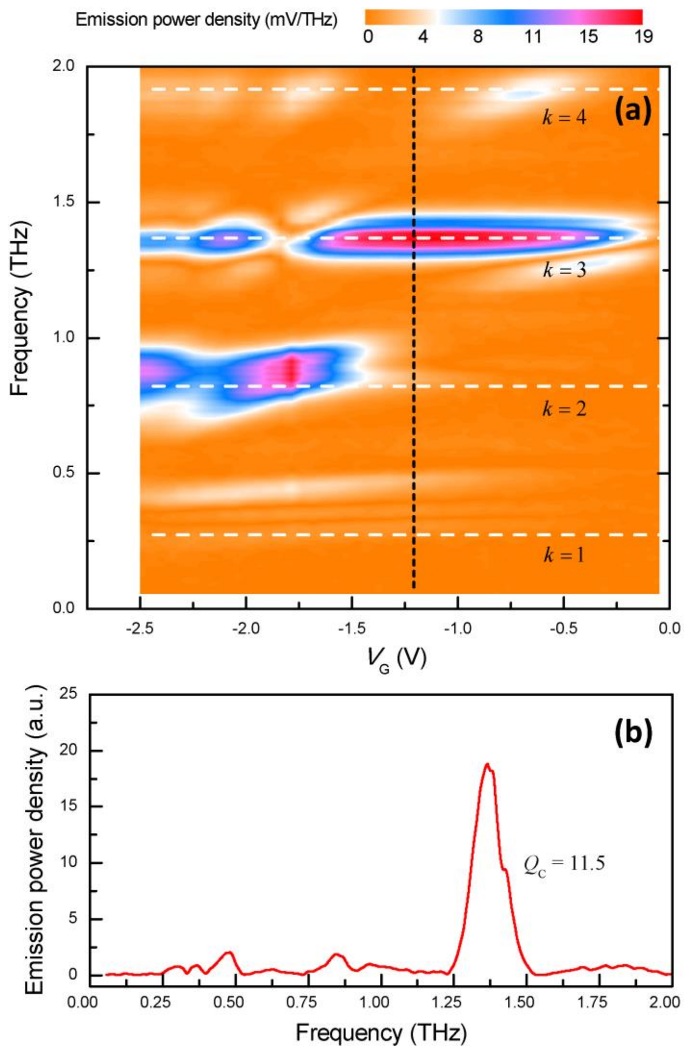

Fig. 5 (a) Emission spectra at different gate voltages. (b) A single emission spectrum at V_G=-1.22 *V*. Obtained from a grating-coupled field-effect transistor with the sapphire substrate thinned down to 91 μm. The device was cooled down to 8 *K*.

The same grating-coupled field-effect transistor is found to be able to emit terahertz wave when it is either biased with a source-drain voltage or controlled by a gate voltage. The detailed mechanism yet needs to be further investigated. However, it is confirmed that such emission originates from plasmon excitation driven by an electrical current injected from the leaky grating gates to the 2DEG instead of a direct source-drain current. As shown in Fig. 5, emission spectra from a similar grating-coupled field-effect transistor at different gate voltages exhibit two bright emission modes (0.85 *THz* and 1.30 *THz*) corresponding to two Fabry-Pérot cavity modes $\omega_{\mathrm{FP}} = (2k-1)\pi c / 2\bar{n}D$ with $k = 1, 2, 3, ...$ and $D \approx 91\ \mu\mathrm{m}$. These terahertz cavity modes are different from Eq. 3 since a reflective mirror is placed on the backside of the sapphire substrate as shown in Fig. 2 (a). A single emission spectrum at $V_{\mathrm{G}} = -1.22\ \mathrm{V}$ is extracted from Fig. 5(a) and is plotted in Fig. 5(b). The full-width-at-half-maximum of the emission peak at 1.37 *THz* is limited by the quality factor ($Q_{\mathrm{C}} \approx 11.5$) of the Fabry-Pérot cavity. Apart from the two bright modes, weaker emission modes are observed from Fig. 5(a). All emission modes are induced from the resonance between the plasmon modes and the Fabry-Pérot cavity modes.

4. Plasmon excitation in an antenna-coupled 2DEG

Plasmon excitation upon incident terahertz electromagnetic wave is probed in the antenna-coupled field-effect transistor as shown in Fig. 2(c) by monitoring the photocurrent at different gate voltages and terahertz frequencies (850, 861, 907 and 940 *GHz*). The channel conductance ($G = \mathrm{d}I_{\mathrm{DS}} / \mathrm{d}V_{\mathrm{DS}}$) as a function of the gate voltage is shown in Fig. 6(a). The threshold gate voltage is about -4.2 *V* and the maximum of transconductance ($\mathrm{d}G / \mathrm{d}V_{\mathrm{G}}$) occurs at -4.0 *V*. Upon coherent terahertz irradiation, a direct photocurrent is induced and is tunable by the gate voltage. As shown in Fig. 6(b), two different types of photo response are observed. One of them have a fixed peak position of -4.0 *V* at which the transconductance is maximized. The peak location of the other response depends on the terahertz frequency. The higher the terahertz frequency, the lower the peak gate voltage, i.e., the higher electron density. The photo responses at -4.0 *V* originate from the non-resonant plasmon excitation while those frequency-dependent responses come from the resonant plasmon excitation. The overall photocurrent can be expressed as a sum of both responses and agrees well with the experiment (solid curves fit well with the experiment data in Fig. 6(b)). The non-resonant plasmon response has been modeled as self-mixing of the incident terahertz electromagnetic wave in the gated 2DEG [20-23]. The resonant plasmon frequency agrees well with the plasmon cavity defined by G2 and G3, as marked by the red area in Fig. 2(c). Such a cavity size ($L_{\mathrm{eff}} = 330\ \mathrm{nm}$) is larger than the length ($L_{\mathrm{G}} = 150\ \mathrm{nm}$) of G1 indicating the plasmon mode is not confined under G1. Instead, the plasmon cavity seems to be defined by G2 and G3 as the boundaries. Such boundaries aren't sharply defined in current device. By extracting the quality factor (Q_{P}) of the resonant plasmon responses as shown in Fig. 6(d), the effective plasmon lifetime ($\tau_{\mathrm{p}} \approx 0.52$ ps) is about 30% of the momentum relaxation time ($\tau_{\mathrm{e}} = \mu m^*/e \approx 1.8$ ps) of the 2DEG indicating the existence of extra damping. It has to be noted that the magnitude of the non-resonant response is much stronger than the resonant response. Since the antenna-coupled field-effect transistor is designed so that the antenna and the gates are symmetric, both resonant and non-resonant responses are suppressed intentionally. However, the fact is that the non-resonant response survives at room temperature while the resonant response dies out quickly when the temperature is increased to about 120 *K*. This fact infers that plasmon in gated 2DEG suffers from strong damping not only from inelastic scattering but also from the leaky boundaries. Once the plasmon cavity is engineered so that the quality factor is lifted up to a few hundreds, one would expect the resonant response becomes the dominating photoresponse and the efficiency of terahertz plasmon emission could be increased too.

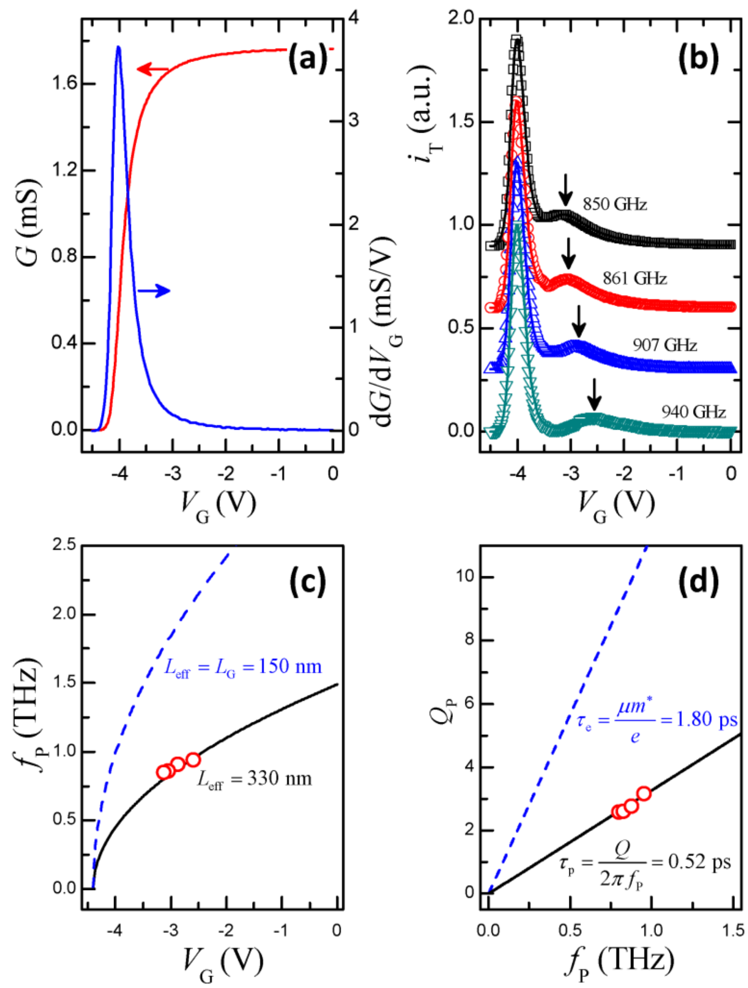

Fig. 6 Resonant and non-resonant plasmon detection in the antenna-coupled field-effect transistor. (a) The channel conductance as a function of the gate voltage VG1. (b) The photocurrent as a function of the gate voltage VG1 at different terahertz frequencies. (c) Extracted resonant frequency as a function of the gate voltage. (d) Extracted quality factor of plasmon modes. The device is cooled down to 77 *K*.

5. Conclusions

In conclusion, terahertz plasmon excitation in AlGaN/GaN 2DEG has been realized both in grating-coupled and antenna-coupled field-effect transistors. Resonant terahertz absorption and electrically-pumped terahertz plasmon emission have been demonstrated in grating-coupled field-effect transistors. Both resonant and non-resonant detection of terahertz electromagnetic wave have been observed in an antenna-coupled field-effect transistor. In both types of devices, plasmons excited no matter by an incident terahertz electromagnetic wave or by electrical power injection are localized plasmons controlled by the gate voltage and hence the local electron density. Furthermore, the damping of localized plasmon modes remains the main hurdle for realizing high-efficiency terahertz devices due to the rather *open* boundaries of plasmon cavities and the limited carrier mobility at room temperature. The efficiency of terahertz plasmon emission and the sensitivity of resonant terahertz plasmon detection could be greatly improved by engineering the boundaries to enhance the quality factor. Terahertz active devices including emitters, detectors and modulators are expected to be realized based on AlGaN/GaN and other high-quality 2DEG materials.

References

[1] R. E. Miles et al. Eds., *Terahertz sources and systems* (Kluwer Academic publishers, Netherlands, 2001).

[2] E. Gornik and D. C. Tsui. "Voltage-tunable far-infrared emission from Si inversion layers". *Phys. Rev. Lett.*, 37, 1425-1428 (1976).

[3] S. J. Allen, D. C. Tsui, and R. A. Logan. "Observation of the two-dimensional plasmon in silicon inversion layers". *Phys. Rev. Lett.*, 38, 980-983 (1977).

[4] U. Mackens, D. Heitmann, L. Prager, et al. "Minigaps in the plasmon dispersion of a two-dimensional electron gas with spatially modulated charge density". *Phys. Rev. Lett.*, 53, 1485 (1984).

[5] R. J. Wilkinson, C. D. Ager, T. Duffield, et al. "Plasmon excitation and self-coupling in a bi-periodically modulated two-dimensional electron gas". *J. Appl. Phys.*, 71, 6049 (1991).

[6] O. R. Matov, O. V. Polischuk, and V. V. Popov. "Electromagnetic emission from two-dimensional plasmons in a semiconductor-dielectric structure with metal grating: Rigorous theory". *International Journal of Infrared and Millimeter Waves*, 14, 1455 (1993).

[7] G. Fasol, N. Mestres, A. Fischer, et al. "Coupled plasmons and single particle excitations in the two-dimensional electron gas". *Physica Scripta.*, T19, 109 (1987).

[8] K. Kempa, P. Bakshi, J. Cen, et al. "Spontaneous generation of plasmons by ballistic electrons". *Phys. Rev. B*, 43, 9273 (1991).

[9] M. Dyakonov and M. Shur. "Shallow water analogy for a ballistic field effect transistor: New mechanism of plasma wave generation by dc current". *Phys. Rev. Lett.*, 71, 2465-2468 (1993).

[10] O. R. Matov, O. V. Polischuk, and V. V. Popov. "Electromagnetic emission from two-dimensional plasmons in a semiconductor-dielectric structure with metal grating: Rigorous theory". *International Journal of Infrared and Millimeter Waves*, 14, 1455 (1993).

[11] K. Hirakawa, M. Grayson, D. C. Tsui, et al. "Blackbody radiation from hot two-dimensional electrons in AlxGa1-xAs/GaAs heterojunctions". *Phys. Rev. B*, 47, R16651 (1993).

[12] K. Hirakawa, K. Yamanaka, M. Grayson, et al. "Farinfrared emission spectroscopy of hot twodimensional plasmons in $Al_{0.3}Ga_{0.7}As$/GaAs heterojunctions". *Appl. Phys. Lett.*, 67, 2326 (1995).

[13] I. E. Tralle, V. A. Sizjuk. "Beam instability and space-charge wave amplification caused by the electron injection out of QW into 2DEG". *physica status solidi (b)*, 196, 85 (1996).

[14] S. A. Mikhailov. "Plasma instability and amplification of electromagnetic waves in low-dimensional electron systems". *Phys. Rev. B*, 58, 1517 (1998).

[15] S. A. Mikhailov. "Tunable solid-state far-infrared sources: New ideas and prspects". *Recent Res. Devel. Applied Phys.*, 2, 65-108 (1999).

[16] P. Bakshi, K. Kempa, A. Scorupsky, et al. "Plasmon-based terahertz emission from quantum well structures". *Appl. Phys. Lett.*, 75, 1685 (1999).

[17] T. Otsuji, T. Watanabe, S. A. B. Tombet, et al. "Emission and detection of terahertz radiation using two-dimensional electrons in III-V semiconductors and graphene". *IEEE Transactions on Terahertz Science and Technology*, 3, 63-71 (2013).

[18] A. Kavokin, J. J. Baumberg, G. Malpuech, et al. *Microcavities* (Oxford University Press, Oxford, 2011).

[19] Y. D. Huang, H. Qin, B. S. Zhang, et al. "Excitation of terahertz plasmon-polariton in a grating coupled two-dimensional electron gas with a Fabry-Pérot cavity". *Appl. Phys. Lett.*, 102, 253106 (2013).

[20] Y. F. Sun, J. D. Sun, Y. Zhou, et al. "Room temperature GaN/AlGaN self-mixing terahertz detector enhanced by resonant antennas". *Appl. Phys. Lett.*, 98, 252103 (2011).

[21] J. D. Sun, Y. F. Sun, D. M. Wu, et al. "High-responsivity, low-noise, room-temperature, self-mixing terahertz detector realized using floating antennas on a GaN-based field-effect transistor". *Appl. Phys. Lett.*, 100, 013506 (2012).

[22] J. D. Sun, H. Qin, R. A. Lewis, et al. "Probing and modeling of localized terahertz self-mixing in a GaN/AlGaN field-effect transistor". *Appl. Phys. Lett.*, 100, 173513 (2012).

[23] J. D. Sun, H. Qin, R. A. Lewis, et al. "The effect of symmetry on resonant and nonresonant photoresponses in a field-effect terahertz detector". *Appl. Phys. Lett.*, 106, 031119 (2015).